



# Post-translational modifications and glycoprofiling of palivizumab by UHPLC–RPLC/HILIC and mass spectrometry

Kulwinder Singh Sran<sup>1</sup> · Yogita Sharma<sup>1</sup> · Tejinder Kaur<sup>1</sup> · Alka Rao<sup>1,2</sup>

Received: 11 February 2022 / Revised: 12 April 2022 / Accepted: 13 April 2022 / Published online: 9 May 2022  
© The Author(s), under exclusive licence to Springer Nature Singapore Pte Ltd. 2022

## Abstract

Viral infections are progressively becoming a global health burden, as witnessed in the ongoing COVID-19 pandemic. Respiratory Syncytial Virus (RSV) is another highly contagious negative-sense RNA virus that causes lower respiratory tract infections and high mortality in infants. Palivizumab (Synagis<sup>®</sup>) is the only humanized monoclonal antibody (mAb) approved by the FDA against RSV. The virus neutralization efficacy often depends on the nature and abundance of the glycoforms in therapeutic mAbs. Therefore, a thorough estimation of their PTM profile, especially glycosylation, is relevant. Here, we describe the intact and released glycan analysis of palivizumab (Synagis<sup>®</sup>) using HILIC chromatography and mass spectrometry. We detected five glycoforms (Man5/G0FB, G0F/G1F, G1F/G1F, G0FB/G0FB, and G2F/G2F) in deconvoluted MS spectra of intact glycosylated palivizumab. The mapping of the peptide and glycopeptides using LC–ESI–MS led to the detection of associated PTMs and the direct identification of a glycopeptide, GlcNAc<sub>3</sub>Man<sub>2</sub>. EEQYNSTYR, derived from the heavy chain of palivizumab. Release glycan analysis using UHPLC–HILIC revealed a typical glycan profile consisting of major glycans, G0F (33.94%), G1F (35.50%), G2F (17.24%) also reported previously and minor G1F' (5.81%), Man5 (3.96%) and G0FB (2.26%) forms with the superior resolution of isomeric G1F/G1F'. Next, we provide the first experimental evidence of Neu5Gc in the commercial palivizumab formulation using DMB labelling. The estimated monosaccharide composition was consistent with previous studies. The findings of the study highlight the efficiency of the release glycan method in providing a correct measure of the total palivizumab glycan pool compared to the intact glycoprotein/glycopeptide approach. The UHPLC–RPLC/HILIC and MS combinations provide a more comprehensive glycoprofile assessment due to the parallel use of fluorescent labels for the analysis of the release of *N*-glycan, sialic acid, and monosaccharide composition. This approach is suitable for quick quality testing and market surveillance of therapeutic mAbs. Alongside a well-perceived need for cost-effective immunoprophylaxis and the ongoing fast-paced development of next-generation variants of palivizumab, such as MEDI8897, the study reiterates glycosylation as a critical parameter that needs monitoring for drug characterization and quality control.

**Keywords** Glycosylation · Therapeutics · Monoclonal antibody · HILIC chromatography

## Introduction

Therapeutic monoclonal antibodies (mAbs) are complex biomolecules due to their molecular size and post-translational modifications of the primary sequence. There are opportunities for post-translational modifications during manufacturing, leading to the introduction of micro-heterogeneity (Schernerman et al. 1999). The US Food and Drug Administration (US FDA) has approved 79 different mAb-based therapeutics, and 570 are currently in the research development stage around the world (Lu et al. 2020). Most therapeutic mAbs are recombinant glycoproteins produced in eukaryotic cells (CHO, NS0, SP2/0) (Sanchez-De Melo

---

Kulwinder Singh Sran and Yogita Sharma contributed equally to this work.

✉ Alka Rao  
raoalka@imtech.res.in

<sup>1</sup> CSIR Institute of Microbial Technology, Sector 39A, Chandigarh 160036, India

<sup>2</sup> Academy of Scientific and Innovation Research (AcSIR), Ghaziabad 201002, India

et al. 2015). These mAbs are expensive because of their high production and characterization cost. Consequently, there is a large market interest in the development of biosimilars for already commercialized innovators. However, these will be offered to the masses at economical prices once the patent expires (Sanchez-De Melo et al. 2015).

Respiratory syncytial virus (RSV) is a frequent cause of lower respiratory infections in infants and children around the world (Bianchini et al. 2020). Like the coronavirus, RSV is a type of respiratory virus, and some symptoms of RSV and COVID-19 can be similar (Subbarao and Mahanty 2020). The World Health Organization (WHO) indicates that more than 90,000 infants are hospitalized with RSV infection, and approximately 325,000 infants are at high risk of developing severe RSV disease in the United States (Schenerman et al. 1999). Table S1 lists different anti-RSV mAbs at various stages of development. Palivizumab (Synagis<sup>®</sup>) is an anti-RSV humanized recombinant mAb (IgG1k) that binds to an epitope at the antigenic site A of the RSV fusion protein (F protein) of RSV (Huang et al. 2010). It consists of 95% human and 5% murine antibody sequences. It has two heavy and two light chains with a molecular weight of approximately 148,000 Da (Schenerman et al. 1999).

Post-translational modifications (PTMs) of therapeutic mAbs are important product quality attributes (PQAs) with potential impact on drug stability, safety, and efficacy. PTMs can occur during mAb production, purification, storage and post-administration. The biopharmaceutical industry desires the control of PQA within predefined acceptance levels to ensure consistent product quality and reduce any impact on drug safety and efficacy (Xu et al. 2017). Glycosylation is one such PQA (tier 2 CQA) of therapeutic mAbs that varies with expression host and manufacturing conditions (Sanchez-De Melo et al. 2015). Evaluation of glycosylation is challenging due to the isomeric and multiantennary nature of glycans (Morelle and Michalski 2006). The guidelines of the European Medicines Agency (EMA) emphasize the use of several orthogonal techniques to identify and quantify glycoforms, glycosylation profiling, and the carbohydrate content of mAbs (Sanchez-De Melo et al. 2015).

Liquid chromatography (LC) and mass spectrometry (MS) techniques are often used to investigate glycosylation directly at the level of intact protein (Sinha et al. 2008) and after proteolytic digestion at the glycopeptide level (Zauner et al. 2010). Although the direct approach is simple and requires minimal processing, it does not accurately measure glycan types and abundance. Therefore, an indirect, more complex, and laborious approach is often employed, where glycans are first released using exoglycosidases, labelled with fluorescent dyes and subsequent analysis using analytical techniques, such as reverse phase liquid chromatography (RPLC), hydrophilic interaction liquid chromatography

(HILIC), capillary electrophoresis (CE) coupled to matrix-assisted laser desorption ionization–mass spectrometry (MALDI–TOF–MS) or electron spray ionization mass spectrometry (ESI–MS). MALDI–TOF–MS has failed to distinguish isobaric/isomeric glycoforms. RPLC cannot retain highly hydrophilic and uncharged glycan species with limited characterization of isomeric glycan structures (Veillon et al. 2017). To overcome these problems, both CE and HILIC coupled with MS have proven to be efficient for glycan studies.

Previous comparative studies involving both techniques have shown a notable complementarity in the glycoform profiling of therapeutic proteins (Virág et al. 2020; Giorgetti et al. 2018). UHPLC–HILIC has high retention power and selectivity for hydrophilic compounds and is efficient in isomer resolution with better retention time repeatability. CE is superior in separating positional isomers and differently linked glycans with high resolution and short analysis time (Kok et al. 2014).

In this study, we used UHPLC–HILIC and mass spectrometry to characterize the PTM profile of palivizumab (Synagis<sup>®</sup>) with a special focus on glycosylation. We have used direct (intact protein and glycopeptide-based) and indirect (release glycan-based) approaches to estimate the glycosylation site, the heterogeneity of glycans and the pool of palivizumab glycans. In addition, the sialic acid and monosaccharide composition of palivizumab were investigated using RP–UHPLC. The analytical approach used provides comprehensive insights into the glycosylation status of palivizumab, which is expected to serve as a viable tool to analyze the differences between glycan profiles of native palivizumab in relation to its various production batches and future biosimilars.

## Materials and methods

### Reagents and chemicals

Palivizumab (Synagis<sup>®</sup> #PZN-10974967) was purchased from Abbvie Deutschland GmbH & Co. KG. Agilent Technologies supplied the 2-AB N-glycan deglycosylation kit (#AT520B5), the AdvanceBio 2-AB Glycan Labelling kit (#5190-8008), the AdvanceBio N-glycan deglycosylation cleanup cartridges (#5190-8007), and the standard N-glycan library (2-AB-Labelled IgG N-linked Glycan library #ATB005007) were supplied by Agilent Technologies. Recombinant PNGase F (#V3021) was supplied by Promega Corporation (Madison, USA). The Signal DMB Labelling Kit (#GKK-407) was purchased from ProZyme. Sodium cyanoborohydride (#25895-60-7), glacial acetic acid (#A6283), formic acid (#8222541001), acetone (#179124), dimethyl sulfoxide (#276855),

ammonium formate (#70221), trypsin (#T6567), 1% sodium metabisulfite (#S1516), Schiff's fuchsin-sulfiteragent (#S5133) and standard sugars, Mannose (#47267), Fucose (#F2252), Galactose (#47267), Glucose (#A8625), were purchased from Sigma-Aldrich. The solvents acetonitrile (ACN), ammonium formate (#70221) and trifluoroacetic acid (TFA, #T1647) used for UHPLC were purchased from Thermo Scientific.

### **Enzymatic deglycosylation of palivizumab and confirmation of deglycosylation using the periodic acid–Schiff (PAS) staining procedure**

Palivizumab was first enzymatically deglycosylated using PNGaseF. 5  $\mu$ l (500  $\mu$ g/675.67  $\mu$ M) of desalted Synagis<sup>®</sup> that harbors approximately 2% glycan (166.6  $\mu$ M), 11  $\mu$ l of 50 mM ammonium bicarbonate buffer and 4  $\mu$ l (10U/ $\mu$ l) PNGaseF were added to the final volume of 20  $\mu$ l. The reaction mixture was incubated at 37 °C for 18 h to achieve deglycosylation. The reaction was stopped by adding 15  $\mu$ l of MilliQ water in 20  $\mu$ l reaction mixture. To confirm deglycosylation and PAS glycoprotein staining, palivizumab samples were run on SDS–PAGE (10%). After the run, the gel was rinsed with distilled water to remove SDS traces and soaked in 50% methanol at room temperature with constant shaking for 30 min. The gel was then washed with 3% acetic acid twice for 20 min each washing. The gel was incubated in an oxidizing solution comprising 1% periodic acid in water for 30 min with constant shaking. After the oxidation step, the gel was washed with 3% acetic acid four times for 20 min each and then incubated in 25 ml of glycoprotein staining solution for 30 min. The glycoprotein stain was decanted, followed by the addition of a reducing agent (1% sodium metabisulphite) and incubation at room temperature for 30 min. The gel was washed several times with 3% acetic acid until the background became clear over the magenta bands. After PAS staining, the gel was counter stained with Coomassie Blue R250.

### **Intact mass analysis of glycosylated and deglycosylated palivizumab using LC–ESI–MS**

mAb deglycosylation was performed as discussed in Sect. 2.2, followed by RPLC using the Advance Bio RP C8 column (Agilent Technologies) operated at 80 °C on the Agilent Infinity LC system consisting of a quaternary pump with a degasser, an auto sampler with a cooling unit and a diode array detector (DAD) coupled to an ESI–QTOF–MS (Agilent 6550 iFunnel Q-TOF–LC–ESI–MS). Before injection, the column was saturated with 90% mobile phase A (0.1% *v/v* formic acid (FA) in MilliQ) and 10% mobile phase B (0.1% *v/v* FA in acetonitrile). The sample (2  $\mu$ l of 1 mg/ml) was loaded

onto the column and separated with a 10–70% gradient of 10–70% of solvent B at a flow rate of 0.5 ml/min for 30 min. Detection was carried out by monitoring UV absorption at 280 nm and TIC was recorded for 1000–7000 *m/z*. The MS parameters applied included capillary voltage 4000 V; sheath gas flow 12, sheath gas temperature 280 °C, gas flow (l/m) 13. A total of 220 MS spectra were calibrated in the positive ion mode and deconvoluted using maximum entropy (MaxEnt) as part of Agilent Mass Hunter Qualitative Analysis (Nupur et al. 2018). MS calibration of the Agilent 6550 iFunnel instrument coupled with a dual Agilent Jet Stream ESI was performed using tuning mix (#G1969-85000 ESI-L).

### **Peptide and glycopeptides mapping of palivizumab using LC–ESI–MS**

Peptide mapping was performed in the reduced tryptic digest of palivizumab to determine the amino acid sequence and possible PTM, including deamidation, oxidation, and glycosylation at Asn297. In-gel palivizumab digestion was carried out according to the manufacturer's instructions. The sample concentration used was 100  $\mu$ g with a 1:50 enzyme to mAb ratio and an enzyme concentration of 1  $\mu$ g/ $\mu$ l. Digestion was performed using MS grade trypsin with overnight incubation at 37 °C. Digested samples were desalted using C18 ZipTip<sup>™</sup> (Millipore Corporation). For MS analysis, the dried digested sample was reconstituted in 0.1% TFA and 10  $\mu$ g of the digested sample was loaded onto the column and analyzed using LC–ESI–QTOF–MS (6550 iFunnel Q-TOF–LC–ESI–MS system equipped with Agilent dualjet stream ESI source). Data analysis was performed using ProteinPilot<sup>™</sup> (AB Sciex) and Byonic software (version v4. 0. 12; Protein Metrics Inc.).

### **Analysis of release glycans through fluorescent 2-AB labelling and detection using UHPLC–HILIC**

The PNGaseF-mediated deglycosylation of Palivizumab was performed as described in Sect. 2.2. After overnight incubation, the released glycans were purified using cleanup cartridges (AdvanceBio N-glycan cleanup cartridges) previously washed with MQ and equilibrated with 96% ACN (2 ml). The sample (35  $\mu$ l deglycosylated reaction mixture + 315  $\mu$ l ACN) was added to the cartridge and drawn to bed level by vacuum followed by washing with 750  $\mu$ l 96% ACN ( $\times$ 3) and elution in 1% formic acid (2 $\times$ 500  $\mu$ l). The eluted fraction was dried in a speed vacuum for 6 h. The purified dry glycan samples were labelled using the AdvanceBio 2-AB Glycan labelling kit. To the dried glycan samples, 1.25  $\mu$ l 2-AB label and 2.5  $\mu$ l reductant (sodium cyanoborohydride) were added. The reaction mixture was incubated at 65 °C for 3 h. After incubation, 8  $\mu$ l MQ and

193  $\mu\text{l}$  100% ACN were added and the labelled glycan samples were cleaned to remove the unbound dye and reductant using cleaning cartridges. The labelled glycans were eluted from the cartridge in MilliQ water ( $2 \times 500 \mu\text{l}$ ), vacuum-dried, and resuspended in 20  $\mu\text{l}$  MilliQ ( $\sim 166.6 \mu\text{M}$  of released glycan). Therefore, the eluted and resuspended 2-AB-labelled glycans were subjected to fluorescence-based detection and quantification.

The relative abundance of glycans was determined by fluorescence detection using HILIC using an AdvanceBio Glycan mapping column ( $2.1 \times 150 \text{ mm}$ ,  $1.8 \mu\text{m}$ , Agilent Technologies) in an Agilent UHPLC system fitted with a flexible pump 1290 Infinity II, 1290 Infinity II vial sampler, 500 nL flow cell of path length 10 mm, 1260 Infinity II DAD (diode array detector) and a fluorescence detector (FLD) set at  $\lambda_{\text{ex}} = 260 \text{ nm}$ ,  $\lambda_{\text{em}} = 430 \text{ nm}$ . The injection was performed with a 2  $\mu\text{l}$  needle ( $\sim 0.5 \mu\text{g}$  or  $16.66 \mu\text{M}$  of released glycan). The mobile phase was composed of 100 mM ammonium formate, pH 4.5 (A) and 100% ACN (B). All instrument operations and data handling operations were managed using Agilent OpenLAB CDS workstation software. The purified 2-AB-labelled glycans were resolved using a 25–60% A gradient for 15 min at a flow rate of 0.5 ml/min, followed by wash and recalibration with a volume of 1 column of mobile phase (Table S7). The column temperature was maintained at  $55 \text{ }^\circ\text{C}$  throughout. The elution profile of 2-AB-labelled palivizumab glycans was compared to the 2-AB-labelled IgG N-linked glycan library. The peaks corresponding to the glycans were manually integrated; annotated and relative abundance was calculated using Agilent OpenLAB CDS data analysis 2.4 software.

### MALDI-TOF mass spectrometry for the qualitative confirmation of 2-AB-labelled glycans

N-glycans labelled with 2-AB were resuspended in 0.1% TFA and analyzed using MALDI-TOF 5800 (AB Sciex). Samples were combined with sinapinic acid (1:1) and spotted on a 384-well MALDI target plate and dried under ambient conditions before analysis. The spectra were acquired in reflectron mode in a mass range of 400–2000 Da. After data acquisition, raw data was extracted in .t2d format and MALDI-TOF-MS spectra were analyzed using Data Explorer v4.9 software (Applied Biosystems). GlycoWorkbench 2.1 software was used to calculate the glycan mass and S/N ratios, manual spectrum matching and draw oligosaccharide structures.

### Analysis of the monosaccharide composition of palivizumab

For the detection of monosaccharides, the constituent monosaccharides were released from the glycans by hydrolysis with 4 M TFA performed at  $80 \text{ }^\circ\text{C}$  for 6 h in a water bath. A set of monosaccharide standards, i.e., mannose, galactose, fucose and glucosamine (GlcNAc) were also treated in the same manner. After being cooled to room temperature, the reaction mixture was evaporated to dryness in a speedvac. The residue was then dissolved in 0.5 ml of methanol and again evaporated to dryness to remove residual TFA (Sran et al. 2019). The dried hydrolyzed monosaccharides and standard sugars were directly labelled with 2-AB (2.5  $\mu\text{l}$  2-AB tag + 2.5  $\mu\text{l}$  Reductant) and incubated at  $65 \text{ }^\circ\text{C}$  for 3 h. The samples were diluted using HPLC running solvent butylamine/orthophosphoric acid/tetrahydrofuran (BPT) and loaded onto the ZORBAX 300SB C18 column ( $4.6 \times 250 \text{ mm}$ ,  $5 \mu\text{m}$ ) with a fluorescence detector ( $\lambda_{\text{ex}} = 360 \text{ nm}$ ,  $\lambda_{\text{em}} = 425 \text{ nm}$ ). The mobile phase solvent composition used is as follows: Solvent A: 0.2% butylamine (2 ml/l), 0.5% phosphoric acid (5 ml/l), 1% tetrahydrofuran (10 ml/l); Solvent B: 50% ACN: 50% solvent A. The method used for the HPLC run is given in Supplementary Table S8.

### Detection of sialic acid moieties in palivizumab

Palivizumab deglycosylation was performed using PNGase F as previously described, followed by purification of the released glycans. Sialic acid was released from the glycan and subsequently labelled with DMB according to the manufacturer's protocol. Separation and detection of DMB-labelled sialic acid was performed using reverse phase UHPLC (Agilent Infinity II) on a ZORBAX 300SB-C18 column (Agilent Technologies,  $4.6 \times 250 \text{ mm}$ ,  $5 \mu\text{m}$ ) column with excitation at 373 nm and emission at 448 nm and the method as given in Supplementary Table S9.

### Secondary structure analysis of palivizumab using Circular Dichroism (CD)

CD was performed to determine the secondary structure of palivizumab using a JASCO J-815 CD spectrometer. The spectra were recorded in the far UV range (200–250 nm) at  $25 \text{ }^\circ\text{C}$  with a spectral bandwidth of 5 nm using a 0.1 cm path length quartz cell at a scan speed of 50 nm/min. The

sample concentration was kept at 100  $\mu\text{g/ml}$ . The far-UV CD signal was converted from millidegrees to mean residue ellipticity using theoretical molecular weight, the number of residues, and protein concentration. Online Dichroweb software was used to estimate secondary structure elements in palivizumab (<http://dichroweb.cryst.bbk.ac.uk/html/home.shtml>).

## Results and discussion

### Confirmation of mAb deglycosylation using PAS staining

The structural elucidation of glycans is challenging because of their isobaric and antennary nature. The traditional approach involves the use of exoglycosidases, such as PNGase F, which selectively and sequentially release terminal sugars, producing trimmed glycans suitable for HPLC analysis. The release of palivizumab glycans was confirmed by PAS staining (Fig. S1A), followed by counterstaining with CBB under reducing conditions (Fig. S1B). As PNGase F is specific for removing *N*-linked glycans; no band corresponding to the deglycosylated mAb was detected in the PAS gel. In contrast, a single band for the glycosylated heavy chain was visible in the native mAb sample. The results indicate the deglycosylation of palivizumab at a conserved glycosylation site in the heavy chain by the PNGase F enzyme. When counterstained with CBB, native palivizumab resolved into two bands with a molecular weight between 50 and 37 kDa for the heavy chain and 25 kDa for the light chain. These results are consistent with the LC–ESI–MS data, as discussed in subsequent sections.

### Intact mass analysis of palivizumab and glycoform identification

The first step to characterize mAb is intact mass measurement by LC–ESI–MS analysis. As a result of the different glycoforms present in palivizumab, the spectra show mass variation in intact palivizumab. MS spectra extracted from the total ion chromatogram (TIC) for the main peak with retention time (RT) at 10.5 min showed the appearance of a typical charge envelope for a protein of high molecular weight. The spectra were less resolved due to the heterogeneity of the glycans and deconvolution resulted in masses corresponding to glycoforms that are Man5/G0FB, G0F/G1F, G1F/G1F, G0FB/G0FB and G2F/G2F. The mass assignment for the detected glycoforms is presented in Table S3. The deconvoluted ESI mass spectra of intact and deglycosylated palivizumab are shown in Fig. 1A, B, respectively. In the present study, the intact mass of glycosylated Palivizumab was found to be 148,285.70 Da, which is consistent with previous reports by Schenerman et al. (1999) and Hiatt et al. (2014) (Table 1). We also measure mass of 145,076.19 Da of deglycosylated palivizumab that is not reported previously. Palivizumab (Synagis® #PZN-10974967) used in the current study contains a total glycan of 2.16%, according to the previous literature (Schenerman et al. 1999).

### Peptide and glycopeptides mapping of palivizumab using LC–ESI–MS

Therapeutic mAbs produced in mammalian cells are heterogeneous due to PTMs, such as glycosylation. Peptide mapping of intact glycoproteins digested with proteolytic enzymes generates valuable information regarding various PTMs present in a protein, such as protein composition, structure, and modification sites. Information on glycan

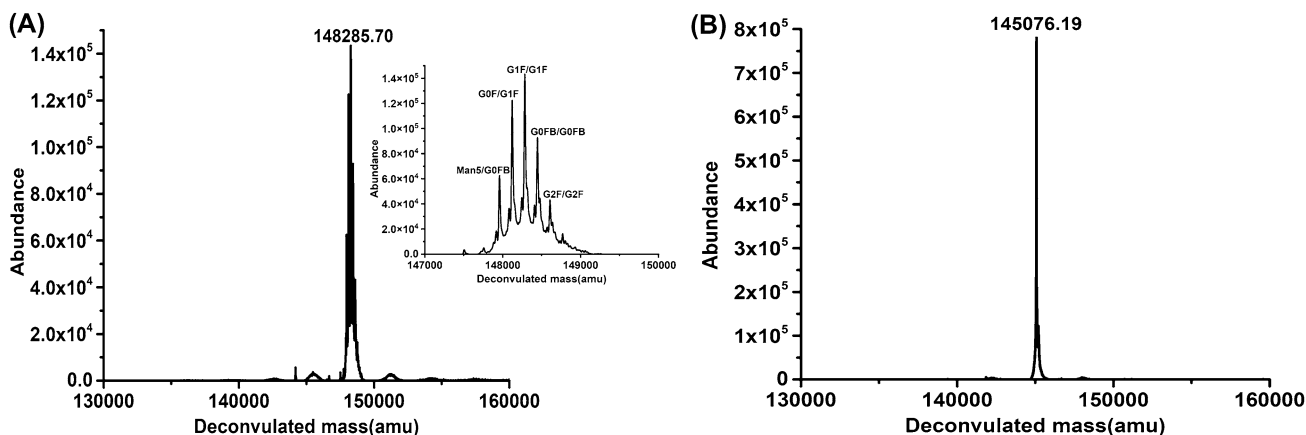


**Fig. 1** Intact mass analysis of palivizumab (Synagis®) using LC–ESI–MS. **A** Deconvoluted mass of glycosylated palivizumab. **B** Deconvoluted mass of deglycosylated palivizumab. The insets in A

show the ionization spectrum. Theoretical mass of palivizumab: 148 kDa, observed: glycosylated mass: 148.285 kDa; Observed: deglycosylated mass: 145.076 kDa

**Table 1** Account of experimentally validated CQA of palivizumab (Synagis®) as collated from published literature

| Critical quality attributes (CQA)          | Schenerman et al. (1999)   | Hiatt et al. (2014)   | Giorgetti et al. (2018)   | Present study (2021) [#PZN-10974967]   |
|--|--|---|---|--|
| <b>Tier 2</b>                              |  |   |   |  |
| Release Glycan Analysis<br>N-linked glycan | Methods: Anion exchange chromatography<br>Glycans identified:<br>G0F<br>Man5/G1F/G1F'(unresolved forms)<br>G2F           | Fluorescent label: 2-AA<br>Methods: Normal Phase HPLC<br>Glycans identified:<br>G0: 5%<br>G0F: 39%<br>G0FB: 5%<br>G1F: 37%<br>G2F: 8% | Fluorescent label: 2-AB<br>Methods: UHPLC–HILIC–FLD and CE–ESI–MS<br>Glycans identified (%):<br>G0F: 29.4 ± 2.9<br>G1F: 44.9 ± 1.5<br>G2F: 13.7 ± 2.5<br>G0F-N: 2.4 ± 0.5<br>G1F-N: 3.0 ± 0.2<br>G0: 0.2 ± 0.1<br>G1: 0.3 ± 0.1<br>G2: 1.2 ± 0.1<br>G0-N: 0.7 ± 0.2<br>G1FS-N: 0.5 ± 0.1<br>G1FS: 0.2 ± 0.1<br>Man5: 3.4 ± 0.5<br>Man6: 0.2 ± 0.1 | Fluorescent label: 2-AB<br>Methods: UHPLC–HILIC–FLD<br>Glycoforms identified (%):<br>G0F: 33.94 ± 2.8<br>Man5: 3.96 ± 0.36<br>G0FB: 2.26 ± 0.26<br>G1F: 35.50 ± 6.46<br>G1F': 5.81 ± 1.03<br>G2F: 17.24 ± 2.73                                 |
| <b>Tier 3</b>                              |  |   |   |  |
| Intact mass                                | Glycosylated:<br>147,700 ± 1000 Da<br>Deglycosylated: NA   | Glycosylated:<br>147,700 ± 1000 Da<br>Deglycosylated: NA  | Glycosylated: NA<br>Deglycosylated: NA  | Glycosylated: 148.285 kDa<br>Deglycosylated: 145.076 kDa   |
| Monosaccharide composition                 | Methods: RPLC PMP Labelling<br>Sugars identified:<br>GlcNAc = 40–60%<br>Man + Gal = 20–45%<br>Fuc = 5–15%<br>Gal = 2–12% | NA  | NA  | Methods: Labelling of UHPLC–HPLC–2AB<br>Sugars identified:<br>GlcNAc 69.73 ± 1.05<br>Fuc 9.16 ± 0.35<br>Man, Gal 21.09 ± 0.72  |
| Sialic acid analysis                       | NA   | NA  | NA  | Neu5Gc (trace amount)  |
| Secondary structure analysis               | NA   | NA  | NA  | β sheet (97%), α-helix (1%) and random coil (2%)   |
| Peptide Mapping                            | Method: RPLC of tryptic digest<br>Modifications detected:<br>Deamidation, Oxidation                                      | NA  | Methods: CE–ESI–MS of tryptic digest<br>Modifications detected:<br>Glycosylation<br>Glycans reported:<br>G0F: 29.2 ± 0.5<br>G1F: 43.5 ± 2.0<br>G2F: 15.7 ± 1.1<br>G0F-N: 2.4 ± 0.2<br>G1F-N: 3.1 ± 0.3<br>G0: 0.2 ± 0.2<br>G1: 0.6 ± 0.2<br>G0-N: 0.8 ± 0.2<br>G1FS-N: 0.5 ± 0.1<br>0.6 ± 0.2<br>G1FS: 0.1 ± 0.1<br>Man5: 3.8 ± 0.5               | Methods: LC–ESI–MS of tryptic digest<br>Modifications: Carbamido methylation (C97; C147; C203; C223; C264; C324; C364), Deamidation (N86; N300; N328), Oxidation (M34; M255), Dioxidation (W49), pyro Glu formation (Q1), Glycosylation (N300) |

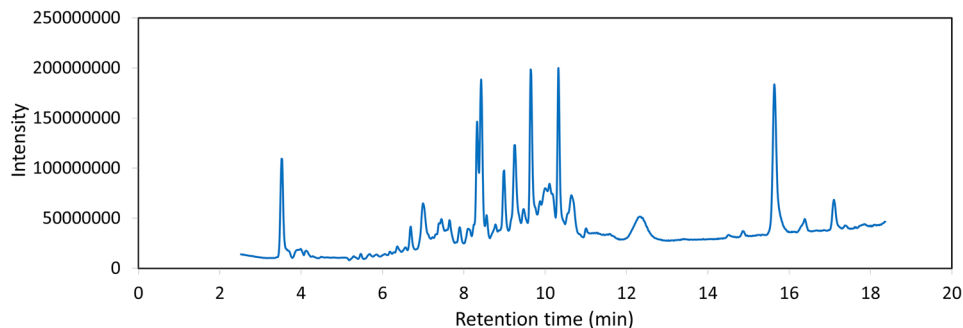
heterogeneity and site occupancy is preserved in peptide mapping (Gilar et al. 2011). Although release glycan analysis is efficient for accurate glycan identification and quantitation, peptide mapping serves as corroborating evidence on the glycosylation features of a protein. Moreover, the

mapping procedure does not require the release and labeling; therefore, the complexity of sample preparation is reduced.

LC–ESI–MS/MS peptide maps of intact-glycosylated and intact-deglycosylated palivizumab generated similar

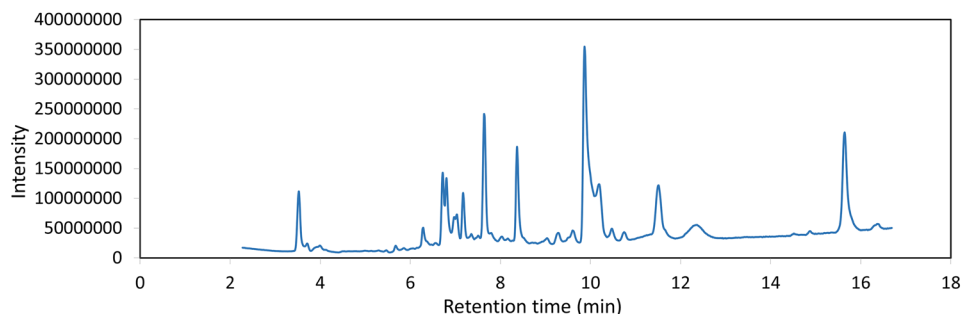
**Fig. 2** LC–ESI–MS chromatogram and sequence coverage map of the glycosylated and deglycosylated heavy chain tryptic digest of palivizumab. Green indicates peptides with at least 95% confidence, yellow with 50% confidence, red with very low confidence, and gray indicates an uncleaved region

### (A) Glycosylated



QVTLRESGPA LVKPTQTLLTCTFSGFSLSTSGMSVGVWIRQPPGKALEWLADIWWDKKDYNPSLKSRLTISKDTSKN  
 QVVLKVTNMDPADTATYYCARSMITNWFYD VWGAGTTVTVSSASTKGPSVFPLAPSSKSTSGGTAALGCLVKDYFPE  
 PVTVSWNSGALTSGVHTFPAVLQSSGLYSLSSVVTVPSSSLGTQTYICNVNHKPSNTKVDKRVPEKSCDKTHTCPPCPA  
 PELLGGPSVFLFPPKPKDTLMISRTPEVTCVVDVSHEDPEVKFNWYVDGVEVHNAKTKPR EEQYNSTYRVVSVLTVL  
 HQDWLNGKEYKCKVSNKALPAPIEKISKAKGQPREPQVYTLPPSREEMTKNQVSLTCLVKGFYPSDIAVEWESNGQP  
 ENNYKTPPVLDSDGSFFLYSKLTVDKSRWQQGNV FSCVMHEALHNNHYTQKSLSLSPGK

### (B) Deglycosylated



QVTLRESGPA LVKPTQTLLTCTFSGFSLSTSGMSVGVWIRQPPGKALEWLADIWWDKKDYNPSLKSRLTISKDTSKN  
 QVVLKVTNMDPADTATYYCARSMITNWFYD VWGAGTTVTVSSASTKGPSVFPLAPSSKSTSGGTAALGCLVKDYFPE  
 PVTVSWNSGALTSGVHTFPAVLQSSGLYSLSSVVTVPSSSLGTQTYICNVNHKPSNTKVDKRVPEKSCDKTHTCPPCPA  
 PELLGGPSVFLFPPKPKDTLMISRTPEVTCVVDVSHEDPEVKFNWYVDGVEVHNAKTKPR EEQYNSTYRVVSVLTVL  
 HQDWLNGKEYKCKVSNKALPAPIEKISKAKGQPREPQVYTLPPSREEMTKNQVSLTCLVKGFYPSDIAVEWESNGQP  
 ENNYKTPPVLDSDGSFFLYSKLTVDKSRWQQGNV FSCVMHEALHNNHYTQKSLSLSPGK

peaks with similar retention time and intensities (Fig. 2). The data analysis using ProteinPilot™ (AB Sciex) showed a sequence coverage of 43.4% in the case of glycosylated samples with a total of 113 peptides with different confidence intervals (17 peptides with > 95%, 25 peptides with > 1%, 71 peptides with < 1%) and 55.9% in the deglycosylated mAb with 107 total peptides (16 peptides with > 95%, 20 peptides with > 1%, 71 peptides with < 1%) compared to a reference amino acid sequence of palivizumab in the database. The data analysis using Bionyc (v4.0.12, Protein metrics) software revealed a lower sequence coverage and lower peptide count compared to ProteinPilot™. 30.4% sequence coverage (51 peptides) for glycosylated and 25.8% (34 peptides) for deglycosylated palivizumab were observed. The modified peptides, together with their PTM modifications, the

sequence of the peptide, and the molecular mass of the peptide are presented in supplementary Tables S4 and S5.

The common modifications detected using both softwares include carbamidomethylation at cysteine residues, deamidation at asparagine residues, pyroglutamate formation, oxidation of methionine, oxidation/dioxidation of tryptophan, and glycosylation (Table S6).

Carbamidomethylation of cysteines is a common modification in mAbs because of the reaction with iodoacetamide, which issued to block cysteine from oxidation. Cysteine residues are highly reactive and can lead to disulfide bond formation in peptides. To prevent them from reacting and forming disulfide links, reduction and alkylation steps were carried out, which resulted in carbamidomethylation of cysteine residues (Rombouts et al. 2013). Carbamidomethylation of multiple cysteine residues (C97; C147; C203;

C223; C264; C324; C364) was observed in palivizumab (Table S6).

Deamidation is a common PTM observed in biopharmaceutical proteins, such as monoclonal antibodies, where the covalent amide functional group gets converted to a carboxylic acid. It usually occurs on asparagine (Asn) or glutamine (Gln) residues to produce aspartic acid (Asp) or glutamic acid (Glu). Deamidation is responsible for the degradation of glycoproteins, and therefore, its characterization is critical to understand their roles in protein stability and disease (Ying and Li 2020). In the present study, the deamidation of asparagine N86, N300, and N328 was observed in the case of palivizumab.

Pyroglutamate (pE) formation, also termed *N*-term cyclization, is another PTM, which affects product quality, safety, and efficacy. The spontaneous cyclization of both glutamine and glutamate at the *N*-termini of recombinant mAbs to pE in vitro, making mAbs acidic and resistant to amino peptidases (Rink et al. 2010) pE, can be one of the many PTM observed during the production and storage of therapeutics such as palivizumab. Ait-Belkacem et al. have reported a modification of pE in the VH domain of palivizumab, occurring through rearrangement of the originally synthesized glutamine residue (Ait-Belkacem et al. 2014). We also detected pE formation at the Q1 position of the variable region of heavy chain in palivizumab.

Oxidation is another common modification that influences the stability and biological functions of therapeutic mAbs. The position of oxidized amino acids in the protein sequence can directly impact the structure of the protein and the binding properties of the antigen receptor (Folzer et al. 2015). Previous studies have reported reduced binding to the neonatal Fc receptor and the biological half-life of concerned mAb due to methionine oxidation in the Fc region (Liu et al. 2008). Furthermore, oxidation of methionine or tryptophan in complementary determining regions (CDRs) can cause loss of potency and antigen binding ability (Folzer et al. 2015). In the current study, methionine oxidation at M34, M255, and tryptophan oxidation at the position W49 in the heavy chain of palivizumab were recorded.

Glycosylation is one of the most heterogeneous PTMs, occurring at a conserved asparagine residue in the fragment crystallizable (Fc) region of mAbs. It can affect the stability of the molecule and interactions with the Fc receptors in vivo. The distribution of glycoforms can affect the mode of action and have implications for drug bioactivity, safety, and efficacy (Giorgetti et al. 2018; Kaur et al. 2021). In the present study, we studied the glycoprofile of palivizumab through release glycan and direct glycopeptide detection methods. The direct glycopeptides coverage obtained using CID-based MSMS fragmentation was found to be poor in our study. We detected a single glycopeptide GlcNAc<sub>3</sub>Man<sub>2</sub>.EEQYNSTYR, derived from the heavy chain

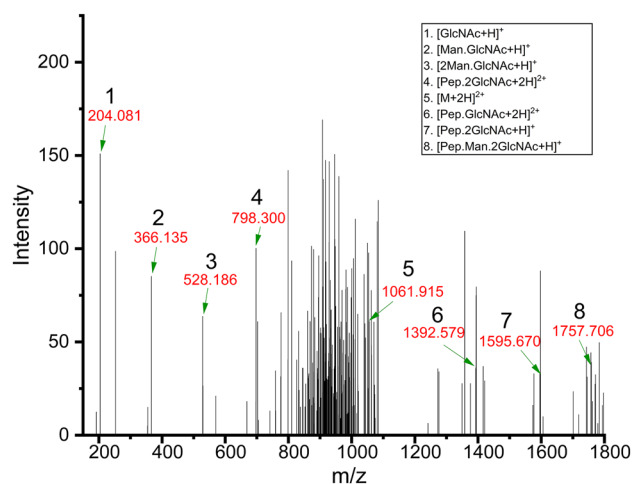


**Fig. 3** CID fragmentation spectrum of the glycopeptide GlcNAc<sub>3</sub>Man<sub>2</sub>.EEQYNSTYR detected in glycosylated palivizumab. Intact peptides (*m/z* 1061) and diagnostic peaks (*m/z* 204, 366 and 528) for GlcNAc and mannose species are visible in the spectrum

of palivizumab, in the glycosylated mAb sample with a low confidence interval (< 1). Figure 3 shows the CID spectrum of the doubly protonated glycopeptide with truncated antennas. The fragmentation pattern shows a peak corresponding to the truncated glycopeptide  $[M + 2H]^{2+}$  with loss of a monosaccharide unit  $[GlcNAc + H]^+$ , observed as a diagnostic peak at *m/z* 204. Giorgetti et al. have reported 11 glycan forms in glycopeptide analysis using CE–ESI–MS (Tables 1 and S2), while the coverage and identification of glycopeptides remained low using LC–ESI–MS in our study (Giorgetti et al. 2018). Previous studies have highlighted the potential of CE–ESI–MS over RPLC–MS in glycopeptide identification (Giorgetti et al. 2018; Chen et al. 2018). Although CE provides better resolution and faster separation time than HPLC methods, the instrumentation and maintenance cost of CE is much higher than that of other analytical machines (Nowak et al. 2020).

### ***N*-linked glycosylation profile of palivizumab by HILIC chromatography**

Glycans typically do not have a chromophore and thus exhibit low absorptivity in both ultraviolet and visible light. Hence, detection systems associated with most analytical techniques require the glycan to be labelled with fluorescent tags that allow high-sensitivity analysis. With the help of reductive amination chemistry, the free reducing end of the glycans is labelled with 2-aminobenzamide (2-AB) or any other fluorescent tag. The resulting tagged glycans can then be separated, identified, and quantified using HPLC and/or MS methods.



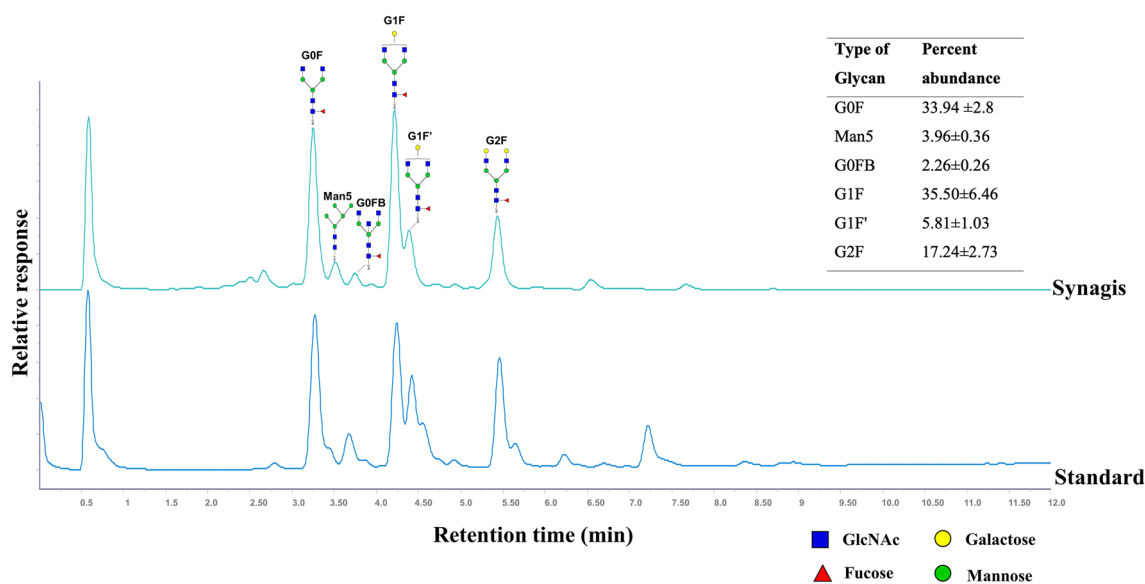


**Fig. 4** UHPLC chromatogram of palivizumab (Synagis®). Overlay of UHPLC chromatograms of palivizumab and 2-AB-labelled glycan standard as detected by the fluorescent detector. The types of

glycans identified and their percent abundance are given in the inset. The Consortium of Functional Glycomics (CFG) nomenclature was adopted to represent glycans

UHPLC–FLD analysis of palivizumab revealed the presence of glycans, namely, G0F, G1F, G1F', G2F, G0FB, and Man5, making it similar to those reported previously (Schenerman et al. 1999; Giorgetti et al. 2018; Hiatt et al. 2014). Tables 1 and S2 list the glycans detected in previous studies and the corresponding relative abundance values. Here we identified six glycan species in the palivizumab formulation with G0F (33.94%), G1F (35.50%), and G2F (17.24%) as the three most abundant and reproducible forms consistently reported in previous reports (Schenerman et al. 1999; Giorgetti et al. 2018; Hiatt et al. 2014) (Fig. 4). The minor glycans G0FB and Man5 were detected with relative abundances of 2.26% and 3.96%, respectively. The occurrence and abundance of minor forms are not consistent between the different reports on palivizumab. Schenerman et al. have reported that the glycan peaks for the Man5 and G1F/G1F' isomeric forms are not resolved properly (Schenerman et al. 1999). Similarly, the G0FB form was previously reported by Hiatt et al. with a relative abundance of 5%. Palivizumab was used in this study, which is produced in the NS0 cell line (Hiatt et al. 2014). Hamm et al. also expressed a recombinant mAb in NS0 cell lines with glycan composition and relative abundance levels similar to those of our study (Table S2) (Hamm et al. 2013).

Furthermore, we were able to resolve isomeric G1F/G1F' glycans successfully; however, these glycoforms have never been widely discussed in the past in the case of palivizumab. Murine cell lines such as NS0 and SP2/0 synthesize galactose glycans in  $\alpha$ -1,3 linkages (Hamm et al. 2013). Varadi et al. have reported the presence of isomeric

G1F/G1F' glycans with galactose linked through  $\alpha$ -1,6 (G1F) and  $\alpha$ -1,3 (G1F') linkages in cetuximab expressed in SP2/0 cells (Váradi et al. 2020). Glycans with  $\alpha$ -1,3-galactose are known to cause an immunogenic response in humans (Hamm et al. 2013). Chung et al. reported a link between hypersensitivity reactions in patients who receive cetuximab drug formulation containing an oligosaccharide, galactose- $\alpha$ -1,3-galactose (Chung et al. 2008). Natural exposure to galactose- $\alpha$ -1,3-galactose might induce IgE production against galactose- $\alpha$ -1,3-galactose in some people, leading to an immunogenic response. Therefore, proper resolution and detailed characterization of isomeric glycoforms such as G1F/G1F' are relevant during the quality assessment of therapeutic mAbs. This linkage has already been described in several NS0-expressed commercial mAbs in the market, with no reported adverse effects (Hamm et al. 2013). These have been discussed in detail in Table S2 and are produced in NS0 cell lines with no reports of adverse effects due to glycans containing  $\alpha$ -1,3-galactose linkage.

The presence of different glycoforms suggested that palivizumab has a heterogeneous population of *N*-glycans and more than 90% of the population is fucosylated. As fucose influences a number of properties, including half-life and cytotoxicity of the drug, fucosylation is an essential factor to consider during the quality assessment of mAb pharmaceutical products. These findings are consistent with previous reports (Kok et al. 2014; Nupur et al. 2018). The present work highlights the efficacy of the HILIC technique in glycan detection with better resolution of the isobaric G1F and

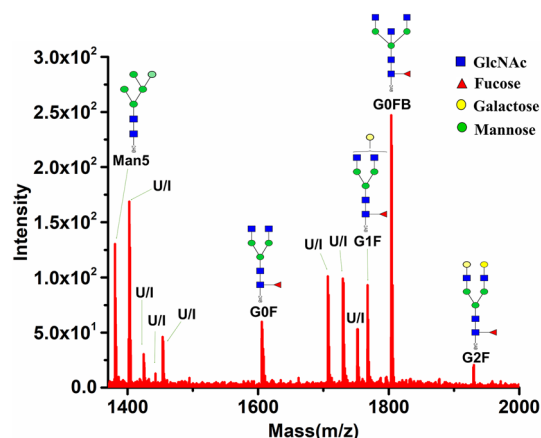


**Fig. 5** MALDI-TOF-MS spectra of *N*-glycan peaks detected in UHPLC. Peaks with *m/z* that do not generate any structure in the glycan database are labelled unidentified (U/I)

G1F' forms of palivizumab by modulating the flow rate (Fig. S2).

Previously, Giorgetti et al. had employed coupled HILIC-MS for release *N*-glycans analysis of different mAbs, including palivizumab (Giorgetti et al. 2018). Using 2-AB labelling we have analyzed the released glycan samples sequentially using UHPLC-HILIC in first step followed by manual peak collection and analysis on MALDI-TOF-MS. The identity of each *N*-glycan peak was manually annotated according to the peak retention time in comparison to known standards. The elucidated *N*-glycan structures are shown above each peak using the conventional glycan nomenclature of the Consortium for Functional Glycomics (CFG). The glycans found in palivizumab are summarized in Fig. 5 (inset) along with their abundance level.

Although overall inline HILIC-MS coupled approach yielded superior results as it involved least sample loss, but, with HILIC alone or sequential HILIC/MS approach here, we could corroborate all the major and minor glycoforms that were first reported by Schenerman et al. (1999) in reproducible manner. This reinforces the reliability, specificity and sensitivity of fluorescent labels and HILIC chromatography in absence of MS.

MALDI-TOF-MS of 2-AB-labelled glycans also corroborated the presence of the glycans listed above. The calculated and observed glycan masses and the corresponding S/N ratio are provided in Table 2. GlycoWorkbench (version 2.1) was used to identify the glycoforms corresponding to their *m/z* (Table 2). There are few *m/z* that do not corroborate any glycan structure and are labelled as unidentified (U/I). Glycan structures annotated in the MALDI-TOF-MS spectrum are shown in Fig. 5.

### Monosaccharide composition of glycans detected in palivizumab

The accurate monomeric composition of a therapeutic mAb provides better insights into their glycosylation status by corroborating the glycan composition of the respective mAb. Therefore, detailed composition analysis is considered an important characteristic for the quality assessment of therapeutic drug products (Schenerman et al. 1999).

The sugar composition of the glycans was analyzed using the UHPLC-FLD method. The results revealed that palivizumab glycan molecules are composed of neutral sugars (mannose, galactose), deoxysugar (fucose), and amino sugars (GlcNAc) (Fig. 6). The presence of different sugar moieties suggests that the detected glycans are heterosaccharides. Among these sugars, N-acetylglucosamine was found to be

**Table 2** List of glycans detected in palivizumab (Synagis®) in this study

| Glycoform | Structures (as 2-AB derivatives) | Calculated mass (Da) | Observed mass (Da) | S/N     |
|-----------|----------------------------------|----------------------|--------------------|---------|
| Man 5     |                                  | 1377.49              | 1380.677           | 986.70  |
| G0F       |                                  | 1605.60              | 1605.522           | 233.95  |
| G1F/G1F'  |                                  | 1767.65              | 1767.572           | 376.53  |
| G2F       |                                  | 1929.72              | 1929.611           | 76.35   |
| G0FB      |                                  | 1808.68              | 1803.800           | 1831.58 |

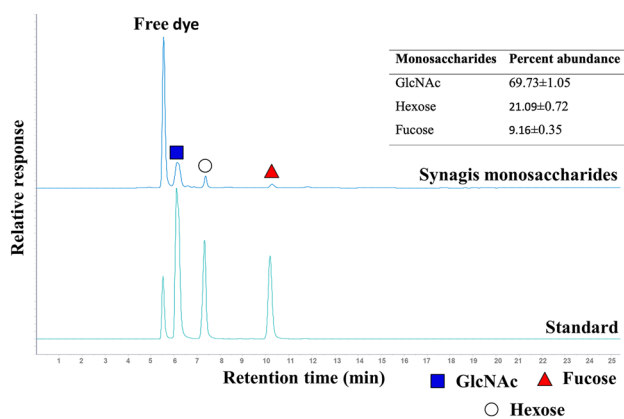


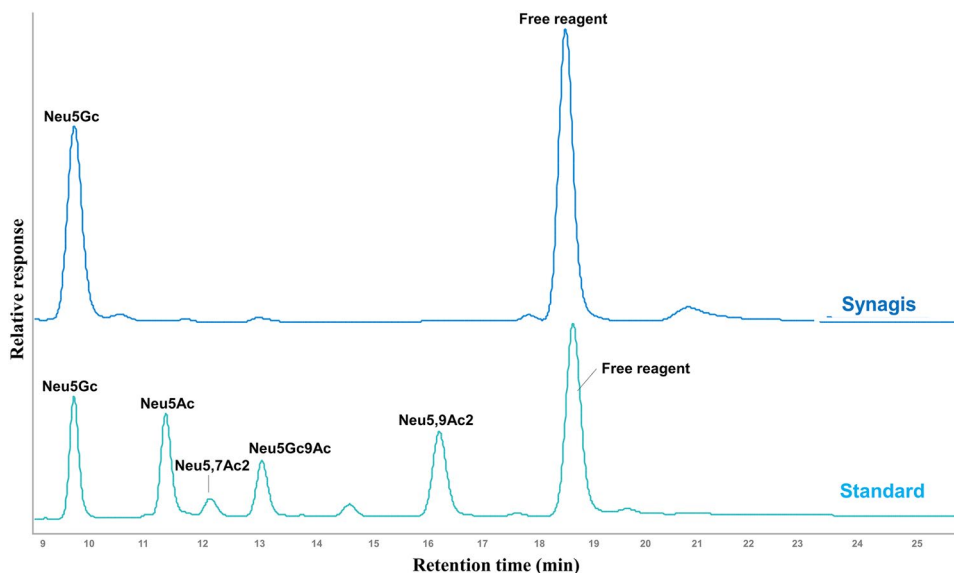
**Fig. 6** Analysis of the sugar composition of the glycan using UHPLC. Overlaid UHPLC chromatogram of 2-AB-labelled standard sugars and 2-AB-labelled released glycan of palivizumab. The spectra chromatogram shows a high abundance of GlcNAc compared to that of other monosaccharides

the most abundant (69.73%) compared to hexoses (21.09%) and deoxy sugar (9.16%), respectively. A significant advantage of 2-AB-labelled monosaccharides is the different elution behaviour of amino sugars as opposed to the other monosaccharides on RPLC.

### Detection of sialic acid in palivizumab using DMB labelling

Sialic acids belong to a family of nine-carbon acidic monosaccharides that occur naturally at the terminal of sugar/glycan chains attached to the glycoprotein. The two most common sialic acids linked to glycans (glycoprotein), i.e., *N*-acetylneuraminic acid (NANA or Neu5Ac) and *N*-glycolylneuraminic acid (NGNA or Neu5Gc) (Ghaderi et al. 2012).

**Fig. 7** UHPLC chromatogram of DMB-labelled sialic acid standard and sialylated glycan species. Neu5Gc (*N*-Glycolylneuraminic acid), Neu5Ac (*N*-Acetylneuraminic acid), Neu5,7Ac2 (*N*-acetyl-7-*O*-acetylneuraminic acid), Neu5Gc9Ac (9-*O*-acetylated-*N*-glycolylneuraminic acid) Neu5,9Ac2 (5-*N*-acetyl-9-*O*-acetyl neuraminic acid)



The form of Neu5Ac sialic acid is found in both human and non-human cells, whereas Neu5Gc is synthesized by all mammalian cells except human cells. The difference in the presence of only one oxygen atom in Neu5Gc from its homologue, Neu5Ac, makes it immunogenic in humans. Furthermore, glycoproteins containing Neu5Gc have been reported to have a reduced serum half-life in patients' blood due to Neu5Gc-specific antibodies (Nguyen et al. 2005). The type of sialic acid and sialylated glycans depends on the host cell expression. Table S2 lists the glycan composition detected in different mAbs produced in mammalian cells, NS0, CHO, and plant sources. CHO cells are reported to express mAbs in the forms of Neu5Ac and Neu5GC sialic acid, while the mAbs produced in NS0 cells contain mainly Neu5Gc forms (Kaur et al. 2021; Hamm et al. 2013; Goh and Ng 2018). Therefore, it is important to accurately monitor both quantitative levels and types of sialic acid during all stages of the product life cycle.

Palivizumab (Synagis<sup>®</sup>) used in this study is expressed in a stable murine myeloma NS0 cell line (Ghaderi et al. 2012). The UHPLC chromatogram of DMB-labelled sialic acid showed only trace levels of Neu5Gc (Fig. 7). Although no report is available on the presence of sialylated forms in palivizumab, Ghaderi et al. have discussed a high chance of Neu5Gc contamination in Palivizumab due to the source of cell lines (Ghaderi et al. 2012). Maeda et al. studied different mAbs for the content of sialic acid and reported the presence of Neu5Gc in another mAb expressed in the NS0 cell line, gemtuzumab, used for the treatment of acute myeloid leukemia (Maeda et al. 2012). Another study on recombinant mAb produced in NS0 cell lines reported the presence of sialic acid in trace levels in antibody clones (Hamm et al. 2013).

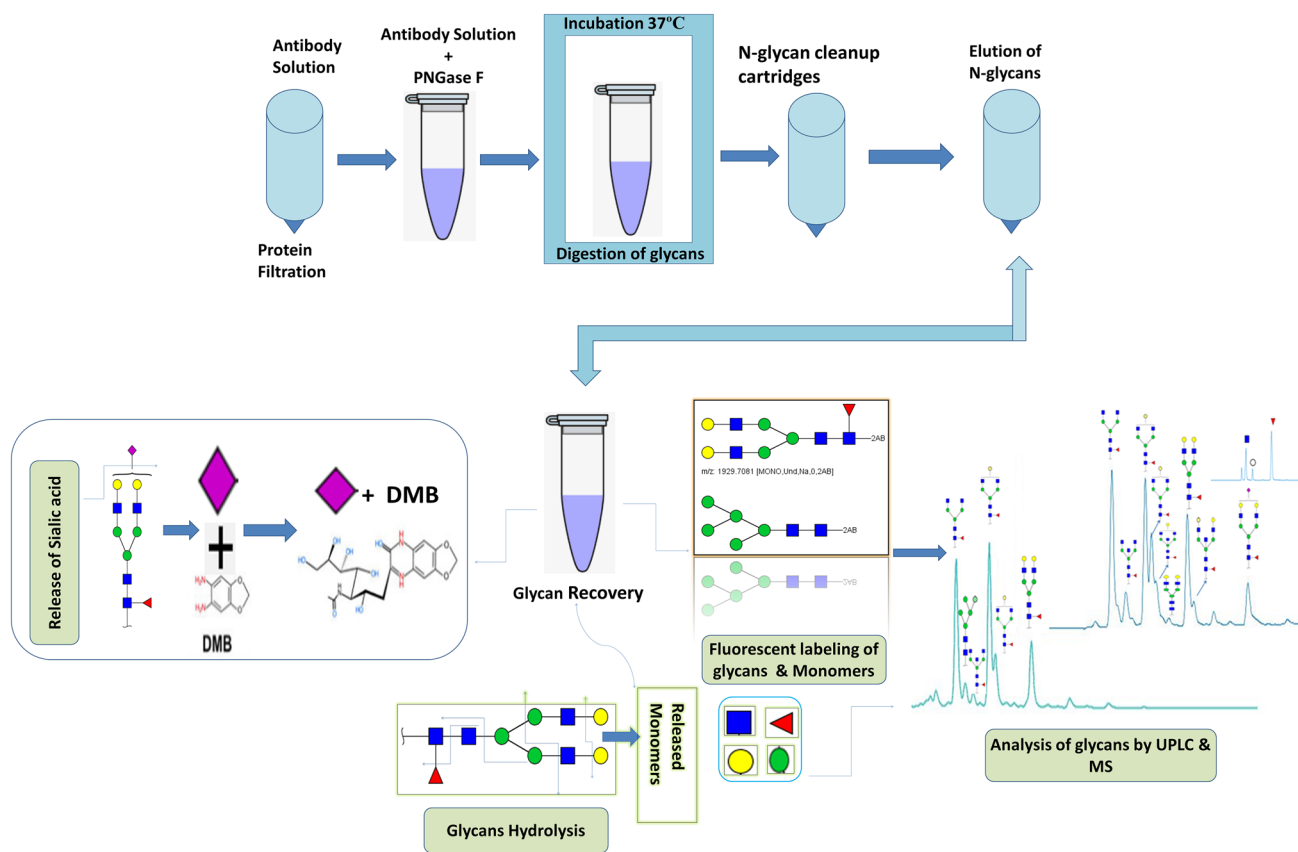


**Fig. 8** Schematic representation of the steps involved in the process of isolation and characterization of *N*-glycans from Palivizumab

### Estimation of secondary structures using CD spectroscopy

Far-UV CD spectroscopy provides information on proteins' secondary structure ( $\alpha$ -helix,  $\beta$ -sheet, and random coil). Estimating the secondary structure of the secondary structure of palivizumab using far-UV CD showed a broad negative drop at 216–218 nm, indicating the expected  $\beta$ -sheet rich structure. The results revealed the presence of  $\beta$  sheet (97%),  $\alpha$ -helix (1%), and random coil (2%) in palivizumab (Fig. S3). Figure 8 shows schematic representation of the steps involved in the process of isolation and characterization of *N*-glycans from Palivizumab.

### Conclusions

The production of therapeutic antibodies with consistent post-translational modifications, mainly the glycosylation patterns remains a challenge in manufacturing. Therefore, monitoring of in-depth glycan profiling of therapeutic mAbs is a critical requirement of such processes. The present study applies both direct (intact glycoprotein/

glycopeptides identification) and indirect (release glycan analysis) approaches to decipher the glycosylation profile of palivizumab (Synagis<sup>®</sup>). We detected five glycoforms, namely, Man5/G0FB, G0F/G1F, G1F/G1F', G0FB/G0FB and G2F/G2F by LC–MS analysis of intact glycosylated palivizumab. Next, we studied the PTM profile of palivizumab through proteolytic digestion of glycosylated and deglycosylated palivizumab. We identified a glycopeptide (EEQYNSTYR) with a truncated glycan on the conserved asparagine residue (N300) on the heavy chain of glycosylated palivizumab. However, inadequate coverage of glycopeptides did not lead to any conclusive evidence on the types of glycans in palivizumab. Therefore, we next performed release glycan studies using the UHPLC–HILIC technique to obtain a correct estimation of palivizumab's glycan pool. We detected six glycoforms, G0F, G1F and G2F being the most abundant and consistent glycoforms in accordance with previous reports. Minor forms, G0FB (2.26%), Man5 (3.96%), and isomeric G1F' (5.81%), are also recorded. The UHPLC–HILIC method is found to be effective in improving the resolution of palivizumab's isobaric glycoforms (G1F and G1F'). These findings highlight the general utility of HILIC for the reproducible

major glycan profiling and specific utility in isomeric glycan profiling of mAbs. In addition, we have shown trace levels of sialic acid (Neu5Gc) in the commercial drug formulation. The estimated monosaccharide composition was consistent with previous studies identifying GlcNAc, fucose, mannose, and galactose as glycan building units.

In conclusion, UHPLC–RPLC/HILIC–MS-based release glycan profiling is efficient in providing reproducible data concerning the major glycan species; therefore, it may be a method of choice for batch processing of therapeutic drug products. Although CE–MS yields superior results for direct glycopeptides mapping, HPLC instrumentation and maintenance is more affordable during bulk sampling. Furthermore, the UHPLC–HILIC–MS combination provide a more comprehensive glycoprofile assessment, because fluorescent labelling can be successfully used for release of N-glycan, sialic acid, and monosaccharide composition analysis (Table 1). Therefore, this approach is suitable for quick quality testing and market surveillance of therapeutic mAbs.

**Supplementary Information** The online version contains supplementary material available at <https://doi.org/10.1007/s42485-022-00086-1>.

**Acknowledgements** The authors thank Dr. Pradeep Sen and Dr. Rajkumar Mehta for facilitating the purchase of palivizumab. The authors thank Ms. Shimona for her helpful suggestions throughout the study and the review of the manuscript.

**Author contributions** The authors confirm the contribution to the paper as follows: Study conception and design: AR; Experimental work: KS, Data analysis and interpretation: KS, YS; Draft manuscript preparation: KS, YS, TK, AR; Revised experiments and data analysis: KS, YS, TK, AR; Review and editing of revised manuscripts: KS, YS, TK, AR.

**Funding** This work is supported by the Council for Scientific and Industrial Research (Grant Nos. MLP-0026 and MLP-0027 to Dr. Alka Rao).

## Declarations

**Conflict of interest** The authors declare that they have no conflict of interest.

## References

Ait-Belkacem R, Berenguer C, Villard C, Ouafik L, Figarella-Branger D, Beck A, Chinot O, Lafitte D (2014) Monitoring therapeutic monoclonal antibodies in brain tumor. *Mabs* 6:1385–1393. <https://doi.org/10.4161/mabs.34405>

Bianchini S, Silvestri E, Argentiero A, Fainardi V, Pisi G, Esposito S (2020) Role of respiratory syncytial virus in pediatric pneumonia. *Microorganisms* 8:1–14. <https://doi.org/10.3390/microorganisms8122048>

Chen C-H, Feng H, Guo R, Li P, Laserna AKC, Ji Y, Ng BH, Li SFY, Khan SH, Paulus A, Chen S-M, Karger AE, Wenz M, Ferrer DL, Huhmer AF, Krupke A (2018) Intact NIST monoclonal antibody characterization—proteoforms, glycoforms—using CE-MS and CE-LIF. *Cogent Chemistry* 4:1480455. <https://doi.org/10.1080/23312009.2018.1480455>

Chung CH, Mirakhor B, Chan E, Le Q-T, Berlin J, Morse M, Murphy BA, Satinover SM, Hosen J, Mauro D, Slebos RJ, Zhou Q, Gold D, Hatley T, Hicklin DJ, Platts-Mills TAE (2008) Cetuximab-induced anaphylaxis and IgE specific for galactose- $\alpha$ -1,3-galactose. *N Engl J Med* 358:1109–1117. <https://doi.org/10.1056/nejmoa074943>

Folzer E, Diepold K, Bomans K, Finkler C, Schmidt R, Bulau P, Huwyler J, Mahler HC, Koulov AV (2015) Selective oxidation of methionine and tryptophan residues in a therapeutic IgG1 molecule. *J Pharm Sci* 104:2824–2831. <https://doi.org/10.1002/jps.24509>

Ghaderi D, Zhang M, Hurtado-Ziola N, Varki A (2012) Production platforms for biotherapeutic glycoproteins. *Occurrence Impact Challeng Non-Hum Sialylat Biotechnol Genetic Eng Rev* 28:147–176. <https://doi.org/10.5661/bger-28-147>

Gilar M, Yu YQ, Ahn J, Xie H, Han H, Ying W, Qian X (2011) Characterization of glycoprotein digests with hydrophilic interaction chromatography and mass spectrometry. *Anal Biochem* 417:80–88. <https://doi.org/10.1016/j.ab.2011.05.028>

Giorgetti J, D'Atri V, Canonge J, Lechner A, Guillaume D, Colas O, Wagner-Rousset E, Beck A, Leize-Wagner E, François YN (2018) Monoclonal antibody N-glycosylation profiling using capillary electrophoresis—mass spectrometry: assessment and method validation. *Talanta* 178:530–537. <https://doi.org/10.1016/j.talanta.2017.09.083>

Goh JB, Ng SK (2018) Impact of host cell line choice on glycan profile. *Crit Rev Biotechnol* 38:851–867. <https://doi.org/10.1080/07388551.2017.1416577>

Hamm M, Wang Y, Rustandi RR (2013) Characterization of N-linked glycosylation in a monoclonal antibody produced in NS0 cells using capillary electrophoresis with laser-induced fluorescence detection. *Pharmaceuticals* 6:393–406. <https://doi.org/10.3390/ph6030393>

Hiatt A, Bohorova N, Bohorov O, Goodman C, Kim D, Pauly MH, Velasco J, Whaley KJ, Piedra PA, Gilbert BE, Zeitlin L (2014) Glycan variants of a respiratory syncytial virus antibody with enhanced effector function and in vivo efficacy. *Proc Natl Acad Sci USA* 111:5992–5997. <https://doi.org/10.1073/pnas.1402458111>

Huang K, Incognito L, Cheng X, Ulbrandt ND, Wu H (2010) Respiratory syncytial virus-neutralizing monoclonal antibodies Motavizumab and Palivizumab inhibit fusion. *J Virol* 84:8132–8140. <https://doi.org/10.1128/jvi.02699-09>

Kaur T, Shukla BN, Yadav VK, Kulkarni MJ, Rao A (2021) Comparison of glycoprofiles of rituximab versions licensed for sale in India and an analytical approach for quality assessment. *J Proteomics* 244:104267. <https://doi.org/10.1016/j.jprot.2021.104267>

Kok MGM, Somsen GW, de Jong GJ (2014) The role of capillary electrophoresis in metabolic profiling studies employing multiple analytical techniques. *Trends Anal Chem* 61:223–235. <https://doi.org/10.1016/j.trac.2014.06.004>

Liu D, Ren D, Huang H, Dankberg J, Rosenfeld R, Cocco MJ, Li L, Brems DN, Remmele RL (2008) Structure and stability changes of human IgG1 Fc as a consequence of methionine oxidation. *Biochemistry* 47:5088–5100. <https://doi.org/10.1021/bi702238b>

- Lu R, Hwang Y, Liu I, Lee C, Tsai H, Li H, Wu H (2020) Development of therapeutic antibodies for the treatment of diseases. *J Biomed Sci*. <https://doi.org/10.1186/s12929-019-0592-z>
- Maeda E, Kita S, Kinoshita M, Urakami K, Hayakawa T, Kakehi K (2012) Analysis of nonhuman N-glycans as the minor constituents in recombinant monoclonal antibody pharmaceuticals. *Anal Chem* 84:2373–2379. <https://doi.org/10.1021/ac300234a>
- Morelle W, Michalski J-C (2006) The mass spectrometric analysis of glycoproteins and their glycan structures. *Curr Anal Chem* 1:29–57. <https://doi.org/10.2174/1573411052948460>
- Nguyen DH, Tangvoranuntakul P, Varki A (2005) Effects of natural human antibodies against a nonhuman sialic acid that metabolically incorporates into activated and malignant immune cells. *J Immunol* 175:228–236. <https://doi.org/10.4049/jimmunol.175.1.228>
- Nowak PM, Sekuła E, Kościelniak P (2020) Assessment and comparison of the overall analytical potential of capillary electrophoresis and high-performance liquid chromatography using the RGB model: How much can we find out? *Chromatographia* 83:1133–1144. <https://doi.org/10.1007/s10337-020-03933-9>
- Nupur N, Chhabra N, Dash R, Rathore AS (2018) Assessment of structural and functional similarity of biosimilar products: rituximab as a case study. *Mabs* 10:143–158. <https://doi.org/10.1080/19420862.2017.1402996>
- Rink R, Arkema-Meter A, Baudoin I, Post E, Kuipers A, Nelemans SA, Akanbi HJ, Moll GN (2010) To protect peptide pharmaceuticals against peptidases. *J Pharmacol Toxicol Methods* 61:210–218. <https://doi.org/10.1016/j.vascn.2010.02.010>
- Rombouts I, Lagrain B, Brunnbauer M, Delcour JA, Koehler P (2013) Improved identification of wheat gluten proteins through alkylation of cysteine residues and peptide-based mass spectrometry. *Sci Rep* 3:1–11. <https://doi.org/10.1038/srep02279>
- Sanchez-De Melo I, Grassi P, Ochoa F, Bolivar J, García-Cózar FJ, Durán-Ruiz MC (2015) N-glycosylation profile analysis of *Trastuzumab* biosimilar candidates by Normal Phase Liquid Chromatography and MALDI-TOF MS approaches. *J Proteom* 127:225–233. <https://doi.org/10.1016/j.jprot.2015.04.012>
- Schenerman MA, Hope JN, Kletke C, Singh JK, Kimura R, Tsao EI, Folena-Wasserman G (1999) Comparability testing of a humanized monoclonal antibody (Synagis®) to support cell line stability, process validation, and scale-up for manufacturing. *Biologicals* 27(3):203–215. <https://doi.org/10.1006/biol.1999.0179>
- Sinha S, Pipes G, Topp EM, Bondarenko PV, Treuheit MJ, Gadgil HS (2008) Comparison of LC and LC/MS methods for quantifying N-glycosylation in recombinant IgGs. *J Am Soc Mass Spectrom* 19:1643–1654. <https://doi.org/10.1016/j.jasms.2008.07.004>
- Sran KS, Sundharam SS, Krishnamurthi S, Roy Choudhury A (2019) Production, characterization and bio-emulsifying activity of a novel thermostable exopolysaccharide produced by a marine strain of *Rhodobacter johrii* CDR-SL 7Cii. *Int J Biol Macromol*. <https://doi.org/10.1016/j.ijbiomac.2019.01.045>
- Subbarao K, Mahanty S (2020) Respiratory virus infections: understanding COVID-19. *Immunity* 52(6):905–909. <https://doi.org/10.1016/j.immuni.2020.05.004>
- Váradí C, Jakes C, Bones J (2020) Analysis of cetuximab N-Glycosylation using multiple fractionation methods and capillary electrophoresis mass spectrometry. *J Pharmaceutical Biomed Anal*. <https://doi.org/10.1016/j.jpba.2019.113035>
- Veillon L, Huang Y, Peng W, Dong X, Cho BG, Mechref Y (2017) Characterization of isomeric glycan structures by LC–MS/MS. *Electrophoresis* 38:2100–2114. <https://doi.org/10.1002/elps.20170042>
- Virág D, Dalmadi-Kiss B, Vékey K, Drahos L, Klebovich I, Antal I, Ludányi K (2020) Current trends in the analysis of post-translational modifications. *Chromatographia* 83:1–10. <https://doi.org/10.1007/s10337-019-03796-9>
- Xu X, Qiu H, Li N (2017) LC–MS multi-attribute method for characterization of biologics. *J Appl Bioanal* 3:21–25. <https://doi.org/10.17145/jab.17.003>
- Ying Y, Li H (2020) Recent progress in the analysis of protein deamidation using mass spectrometry. *Methods*. <https://doi.org/10.1016/j.ymeth.2020.06.009>
- Zauner G, Koeleman CAM, Deelder AM, Wührer M (2010) Protein glycosylation analysis by HILIC-LCMS of proteinase K-generated N- and oglycopeptides. *J Sep Sci* 33:903–910. <https://doi.org/10.1002/jssc.200900850>

**Publisher's Note** Springer Nature remains neutral with regard to jurisdictional claims in published maps and institutional affiliations.